ChemComm

COMMUNICATION

View Article Online
View Journal | View Issue

Combined plasmonic and upconversion rear reflectors for efficient dye-sensitized solar cells†

Cite this: *Chem. Commun.*, 2014, 50, 879

Received 24th September 2013,
Accepted 28th October 2013

DOI: 10.1039/c3cc47290f

www.rsc.org/chemcomm

Parthiban Ramasamy and Jinkwon Kim*

A novel rear reflector structure that combines NIR light harvesting β-$NaGdF_4$:Yb, Er, Fe upconversion nanoparticles (UCNPs) and light reflecting silver particles has been successfully used to improve the performance of dye-sensitized solar cells (DSSCs). The power conversion efficiency of DSSCs with a rear reflector was 7.04%, which is an increase of 21.3% compared to the cell without a rear reflector (5.8%).

Dye-sensitized solar cells (DSSCs) have been considered as some of the most promising candidates to replace conventional silicon based solar cells due to their low cost, easy fabrication, and high efficiencies.[1–3] A typical DSSC consists of a dye-sensitized nanocrystalline TiO_2 semiconductor film on transparent conductive oxide (TCO) glass, an electrolyte solution containing a I^-/I_3^- redox couple, and a platinum coated TCO glass as a counter electrode. A major factor limiting the performance of DSSCs is the light harvesting ability of the sensitizers. Even the most successful sensitizers such as N3, N-719, and N-749 can absorb light with wavelengths in a range between 300 and 800 nm.[4,5] Meanwhile, most of the solar infrared (IR) and near-infrared (NIR) regions, which collect almost half of the energy of the sun's radiation, have not been utilized by these sensitizers. Much effort is now devoted to develop strategies to utilize the IR and NIR parts of sunlight in DSSCs. In order to utilize the NIR light, new sensitizers such as osmium(II) complexes, synthetic organic dyes, and quantum dots have been explored.[6–8] Panchromatic sensitizers were developed to utilize the NIR region, but the poor electron injection efficiency and competing charge recombination of the sensitizers hampered their application.[9]

An alternative strategy is the application of upconversion nanoparticles (UCNPs) for enhancing the light harvesting efficiency in DSSCs. Upconversion is a unique type of photoluminescence in which lower-energy excitation (near-infrared light) is converted into higher-energy emission (visible light), and has been considered as one of the promising solutions to improve the performance of solar cells.[10–12] For example, Wild *et al.* demonstrated the application of β-$NaYF_4$:Yb^{3+}, Er^{3+} upconversion phosphor in an amorphous silicon solar cell. An enhancement of 10 μA cm^{-2} was obtained under illumination with a 980 nm diode laser (10 mW).[13] Shan and Demopoulos reported for the first time application of a TiO_2–UC (Yb, Er^{3+} co-doped LaF^3) nanocomposite working electrode to improve the NIR light harvesting in dye-sensitized solar cells.[14] However, the overall efficiency of the DSSCs decreased due to apparent charge recombination at the UCNP/dye/electrolyte interfaces. Recently, Liang *et al.* reported 29% enhancement in efficiency by using double-shell β-$NaYF_4$:Yb^{3+}, Er^{3+}/SiO_2/TiO_2 submicroplates as scattering and upconverting layers in dye-sensitized solar cells.[15] However, the thickness of the transparent TiO_2 film was increased from 9 to 15 μm, which is one of the critical factors affecting the overall efficiency of the DSSCs.

In this communication, we report a new strategy to improve the efficiency of dye-sensitized solar cells by using external NIR light harvesting and light-reflecting bifunctional layers consisting of upconversion nanoparticles combined with silver particles. The upconversion nanoparticles can absorb NIR light and radiate visible upconverted emission, which can be absorbed by the N719 dye and more photoinduced electrons can be produced to increase the efficiency of DSSCs. Silver particles can function as a back reflector for the upconverted visible photons emitted from the UCNPs bouncing back into the DSSC. In addition silver particles can enhance the upconversion luminescence by the plasmonic effect. The DSSC with a plasmonic and upconversion rear reflector shows a conversion efficiency of 7.04% under one sun illumination, which is an increase of 21.3% compared to the cell without a rear reflector (5.8%). The proposed schematic diagram of the DSSC is shown in Scheme 1.

The upconversion nanoparticles used in this study were 30 mol% Fe^{3+} doped $NaGdF_4$:Yb, Er (18, 2%). In our previous report we found that the Fe^{3+} doped upconversion nanoparticles have 30 times more upconversion luminescence than the undoped UCNPs.[16] The enhanced upconversion luminescence in Fe^{3+} doped UCNPs can be more beneficial for solar cell applications.

Department of Chemistry and GETRC, Kongju National University, 182, Shinkwondong, Kongju, 314-701, Chungnam-do, Republic of Korea. E-mail: jkim@kongju.ac.kr; Fax: +82-41-850-8613; Tel: +82-41-850-8496

† Electronic supplementary information (ESI) available: Detailed experimental procedure, SEM images, XRD patterns, and UV-vis absorption spectra of silver particles. See DOI: 10.1039/c3cc47290f

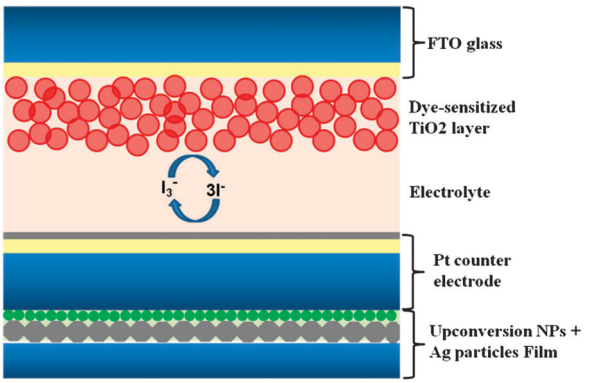

Scheme 1 Schematic diagram of DSSCs with upconversion and plasmonic rear reflector film.

Oleate-capped UCNPs were synthesized from the corresponding rare-earth chlorides using oleic acid as the coordinating ligand and 1-octadecene as the non-coordinating solvent at 300 °C. A detailed experimental procedure is given in the ESI.† Fig. 1a and b show the TEM images of the synthesized UCNPs. The nanoparticles were nearly monodisperse with spherical-like morphology. The average size of the nanoparticles was 20 nm. Fig. 1c shows the XRD pattern of the UCNPs and all the major diffraction peaks can be indexed to the hexagonal β-$NaGdF_4$ (JCPDS card no. 27-0699). The room temperature upconversion emission spectrum of $NaGdF_4$:Yb, Er, Fe (18, 2, 30 mol%) nanoparticles under 980 nm laser excitation is shown in Fig. 1d. The nanoparticles exhibit bright green upconversion luminescence which can be clearly seen by the naked eye (inset in Fig. 1d). The spectrum consists of three distinct bands in the range of 500–700 nm. Two green emissions ranging from 517 to 532 nm and from 532 to 551 nm were attributed to the $^2H_{11/2} \rightarrow {}^4I_{15/2}$ and $^4S_{3/2} \rightarrow {}^4I_{15/2}$ transitions, respectively; the red emission from 635 to 670 nm was due to the $^4F_{9/2} \rightarrow {}^4I_{15/2}$ transition.

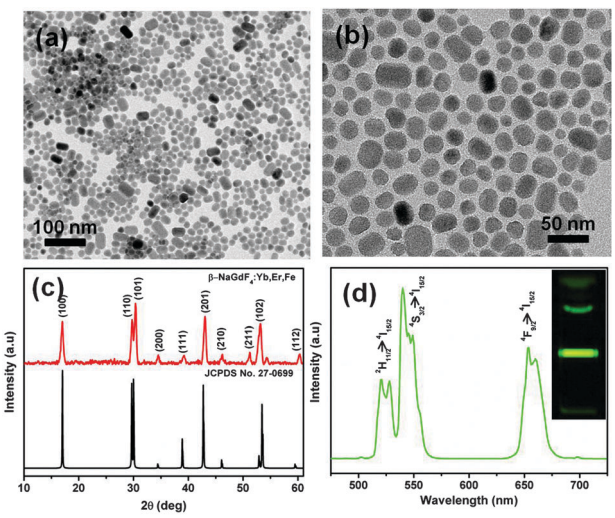

Fig. 1 (a and b) TEM images, (c) XRD patterns, and (d) upconversion photoluminescence spectra of β-$NaGdF_4$:Yb, Er, Fe nanoparticles. Digital photograph of the upconversion fluorescence of β-$NaYF_4$:Yb, Er, Fe NPs in toluene (inset).

Two different sizes of silver particles were synthesized to study the light reflection properties of plasmonic structures. Firstly, 150 nm silver particles (Ag-150) were prepared by the polyol reduction method.[17] Secondly, silver particles with average size of 1 μm (Ag-1000) were synthesized by reducing silver nitrate with ascorbic acid in aqueous solutions.[18] The morphology of these particles was investigated by scanning electron microscopy (SEM) and the images are shown in Fig. S1 (ESI†). The particles synthesized by the polyol method were smaller in size and had a smooth surface; whereas the ascorbic acid reduction method yielded larger particles with a highly roughened surface. The crystal structure and the phase composition of these particles were characterized by XRD. Fig. S2 (ESI†) shows a typical XRD pattern of the as-prepared product. All the peaks can be indexed to face-centered cubic silver (JCPDS No. 04-0783).

Five different light reflection films with different compositions were prepared and tested. The compositions of the films are as follows: UCNPs (RR-01), Ag-150 (RR-02), Ag-150 + UCNPs (RR-03), Ag-1000 (RR-04), Ag-1000 + UCNPs (RR-05). Light scattering properties of the reflector films were evaluated by measuring the diffuse reflectance. As shown in Fig. 2a, film with bigger silver particles (RR-04) has higher reflectance than the smaller silver particle film (RR-02) and UCNP film. Addition of upconversion nanoparticles to the silver films decreased the reflectance little. Upconversion photoluminescence spectra of the rear reflector films are shown in Fig. 2b. The presence of silver particles enhanced the upconversion emission intensities of $NaGdF_4$:Yb, Er, Fe nanoparticles. The enhancement factor is calculated to be 3.1 and 2.2 times for green and red emission, respectively, according to the ratio of the integrated intensity. The enhancement effect from the silver particles may be attributed to at least two possible factors. (1) Increase of the emission rate by surface plasmon-coupled emission (SPCE).[19] SPCE can occur when the emission band of the luminophore overlaps with the plasmon resonance, which will effectively increase both the radiative and nonradiative decay rate. The UV-vis spectra of the silver particles (Fig. S3, ESI†) clearly show that the plasmonic resonance frequency of the silver particles overlaps well with the green and red emission of the upconversion nanoparticles. This allows the effective coupling of silver surface plasmon resonance with upconversion emission, and thus increases the radiative decay rate and emission intensity of the nanoparticles. (2) Increase in emission intensity due to the larger scattering efficiency of the silver particles.[20,21] The larger

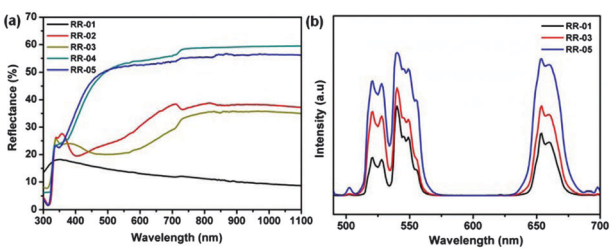

Fig. 2 Diffuse reflectance and upconversion photoluminescence emission spectra of rear reflector films.

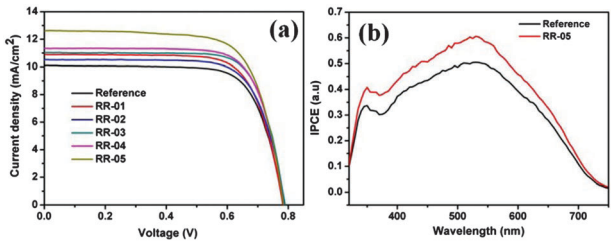

Fig. 3 (a) *J–V* curves, and (b) IPCE spectra of DSSCs with different rear reflector films.

Table 1 Photovoltaic characteristics of DSSCs with different rear reflector films

Device	J_{sc} (mA cm^{-2})	V_{oc} (V)	FF	η (%)
Reference	10.10	0.782	0.73	5.807
RR-01	10.89	0.782	0.73	6.222
RR-02	10.51	0.789	0.73	6.063
RR-03	11.03	0.790	0.74	6.537
RR-04	11.32	0.785	0.74	6.609
RR-05	12.62	0.785	0.71	7.049

silver particles (Ag-1000) have a very rough surface which can scatter the light more effectively than the smaller silver nanoparticles (Ag-150). This explains the upconversion emission enhancement difference between the two different silver particles.

Different rear reflector films were attached externally to the counter electrode of the DSSC and their photovoltaic performance were characterized. Fig. 3 shows the photocurrent density–voltage (*J–V*) characteristics of DSSCs with various rear reflector films measured under standard AM1.5G one-sun irradiation (100 mW cm^{-2}); and their photovoltaic parameters are summarized in Table 1. It can be observed that the short-circuit current density (J_{sc}) and efficiency (η) have increased in all the DSSCs with external reflector films. The open-circuit voltage (V_{oc}) and the fill factor (FF) of the DSSCs were almost the same for all the rear reflector films. For the DSSC with only UCNP rear reflector (RR-01) the enhancement is very little due to the poor light reflection property of the small nanoparticles and the enhancement mainly comes from the NIR light harvesting by the UCNPs. However, the performance of the DSSCs can be further improved by the addition of light reflecting silver particles to the rear reflector films. The DSSC with rear reflector film RR-05 (Ag-1000 + UCNPs) achieved the highest J_{sc} of 12.62 mA cm^{-2}, which was 24.9% greater than 10.1 mA cm^{-2} of the DSSC without any rear reflector. The highest efficiency of 7.04% was achieved, which is about 21.3% higher than that of the device without a rear reflector. The efficiency enhancement is attributed to combination of both the light reflective action of silver particles and NIR light harvesting properties of the upconversion nanoparticles. The incident photon to current conversion efficiency (IPCE) spectra are shown in Fig. 3b. The IPCE of the DSSC with rear reflector RR-05 is higher than that of the DSSC without a rear reflector over the entire wavelength region, which correlates well with the aforementioned higher J_{sc} for the former, indicating that more photocurrent was generated by applying the rear reflectors.

In summary, we have demonstrated improved power conversion efficiency in DSSCs using a back reflector structure that combines upconversion nanoparticles to harvest NIR light and plasmonic silver particles to scatter light. The upconversion photoluminescence of the UCNPs was enhanced 3 times by silver particles. The enhancement is due to surface plasmon-coupled emission and large scattering efficiency of silver particles. DSSCs employing this back reflector structure achieved an efficiency of 7.04%, which is about 21.3% higher than that of the device without a back reflector. The improved device performance is due to NIR harvesting and efficient light reflecting properties of the rear reflector film.

This work was supported by the Priority Research Center Program (2012-0006682) and Basic Science Research Program (2012R1A1A2043731) through the National Research. We thank Dr Sang-Il Seok of Korea Research Institute of Chemical Technology (KRICT) for recording the IPCE spectra.

Notes and references

1 B. O'Regan and M. Gratzel, *Nature*, 1991, **353**, 737–740.
2 A. Hagfeldt, G. Boschloo, L. Sun, L. Kloo and H. Pettersson, *Chem. Rev.*, 2010, **110**, 6595–6663.
3 H. Pettersson, K. Nonomura, L. Kloo and A. Hagfeldt, *Energy Environ. Sci.*, 2012, **5**, 7376–7380.
4 T. W. Hamann, R. A. Jensen, A. B. F. Martinson, H. Van Ryswyk and J. T. Hupp, *Energy Environ. Sci.*, 2008, **1**, 66–78.
5 K. Lee, S. W. Park, M. J. Ko, K. Kim and N. G. Park, *Nat. Mater.*, 2009, **8**, 665–671.
6 K.-L. Wu, S.-T. Ho, C.-C. Chou, Y.-C. Chang, H.-A. Pan, Y. Chi and P.-T. Chou, *Angew. Chem., Int. Ed.*, 2012, **51**, 5642–5646.
7 A. Mishra, M. K. R. Fischer and P. Bäuerle, *Angew. Chem., Int. Ed.*, 2009, **48**, 2474–2499.
8 Z. Pan, K. Zhao, J. Wang, H. Zhang, Y. Feng and X. Zhong, *ACS Nano*, 2013, **7**, 5215–5222.
9 Z. Ning, Y. Fu and H. Tian, *Energy Environ. Sci.*, 2010, **3**, 1170–1181.
10 M. Haase and H. Schäfer, *Angew. Chem., Int. Ed.*, 2011, **50**, 5808–5829.
11 H.-Q. Wang, M. Batentschuk, A. Osvet, L. Pinna and C. J. Brabec, *Adv. Mater.*, 2011, **23**, 2675–2680.
12 B. M. van der Ende, L. Aarts and A. Meijerink, *Phys. Chem. Chem. Phys.*, 2009, **11**, 11081–11095.
13 J. de Wild, A. Meijerink, J. K. Rath, W. G. J. H. M. van Sark and R. E. I. Schropp, *Sol. Energy Mater. Sol. Cells*, 2010, **94**, 1919–1922.
14 G.-B. Shan and G. P. Demopoulos, *Adv. Mater.*, 2010, **22**, 4373–4377.
15 L. Liang, Y. Liu and X.-Z. Zhao, *Chem. Commun.*, 2013, **49**, 3958–3960.
16 P. Ramasamy, P. Chandra, S. W. Rhee and J. Kim, *Nanoscale*, 2013, **5**, 8711–8717.
17 B. Wiley, Y. Sun and Y. Xia, *Acc. Chem. Res.*, 2007, **40**, 1067–1076.
18 H. Liang, Z. Li, W. Wang, Y. Wu and H. Xu, *Adv. Mater.*, 2009, **21**, 4614–4618.
19 H. Zhang, Y. Li, I. A. Ivanov, Y. Qu, Y. Huang and X. Duan, *Angew. Chem., Int. Ed.*, 2010, **49**, 2865–2868.
20 J. R. Lakowicz, *Anal. Biochem.*, 2005, **337**, 171–194.
21 W. Feng, L.-D. Sun and C.-H. Yan, *Chem. Commun.*, 2009, 4393–4395.